AMERICAN SOCIETY FOR MICROBIOLOGY | Journal of Virology®

VACCINES AND ANTIVIRAL AGENTS

Structure-Based Design of Hepatitis C Virus Vaccines That Elicit Neutralizing Antibody Responses to a Conserved Epitope

Brian G. Pierce,[a,b] Elisabeth N. Boucher,[c*] Kurt H. Piepenbrink,[d*] Monir Ejemel,[c] Chelsea A. Rapp,[d] William D. Thomas, Jr.,[c*] Eric J. Sundberg,[d,e] Zhiping Weng,[a] Yang Wang[c]

Program in Bioinformatics and Integrative Biology, University of Massachusetts Medical School, Worcester, Massachusetts, USA[a]; University of Maryland Institute for Bioscience and Biotechnology Research, Rockville, Maryland, USA[b]; MassBiologics, University of Massachusetts Medical School, Boston, Massachusetts, USA[c]; Institute of Human Virology, University of Maryland School of Medicine, Baltimore, Maryland, USA[d]; Departments of Medicine and of Microbiology & Immunology, University of Maryland School of Medicine, Baltimore, Maryland, USA[e]

ABSTRACT Despite recent advances in therapeutic options, hepatitis C virus (HCV) remains a severe global disease burden, and a vaccine can substantially reduce its incidence. Due to its extremely high sequence variability, HCV can readily escape the immune response; thus, an effective vaccine must target conserved, functionally important epitopes. Using the structure of a broadly neutralizing antibody in complex with a conserved linear epitope from the HCV E2 envelope glycoprotein (residues 412 to 423; epitope I), we performed structure-based design of immunogens to induce antibody responses to this epitope. This resulted in epitope-based immunogens based on a cyclic defensin protein, as well as a bivalent immunogen with two copies of the epitope on the E2 surface. We solved the X-ray structure of a cyclic immunogen in complex with the HCV1 antibody and confirmed preservation of the epitope conformation and the HCV1 interface. Mice vaccinated with our designed immunogens produced robust antibody responses to epitope I, and their serum could neutralize HCV. Notably, the cyclic designs induced greater epitope-specific responses and neutralization than the native peptide epitope. Beyond successfully designing several novel HCV immunogens, this study demonstrates the principle that neutralizing anti-HCV antibodies can be induced by epitope-based, engineered vaccines and provides the basis for further efforts in structure-based design of HCV vaccines.

IMPORTANCE Hepatitis C virus is a leading cause of liver disease and liver cancer, with approximately 3% of the world's population infected. To combat this virus, an effective vaccine would have distinct advantages over current therapeutic options, yet experimental vaccines have not been successful to date, due in part to the virus's high sequence variability leading to immune escape. In this study, we rationally designed several vaccine immunogens based on the structure of a conserved epitope that is the target of broadly neutralizing antibodies. *In vivo* results in mice indicated that these antigens elicited epitope-specific neutralizing antibodies, with various degrees of potency and breadth. These promising results suggest that a rational design approach can be used to generate an effective vaccine for this virus.

KEYWORDS hepatitis C virus, immunogen, neutralizing antibodies, protein design, vaccines

Received 22 June 2017 **Accepted** 1 August 2017

Accepted manuscript posted online 9 August 2017

Citation Pierce BG, Boucher EN, Piepenbrink KH, Ejemel M, Rapp CA, Thomas WD, Jr, Sundberg EJ, Weng Z, Wang Y. 2017. Structure-based design of hepatitis C virus vaccines that elicit neutralizing antibody responses to a conserved epitope. J Virol 91:e01032-17. https://doi.org/10.1128/JVI.01032-17.

Editor Michael S. Diamond, Washington University School of Medicine

Address correspondence to Brian G. Pierce, pierce@umd.edu, or Yang Wang, yang.wang@umassmed.edu.

* Present address: Elisabeth N. Boucher, Sartorius Stedim BioOutsource, Cambridge, Massachusetts, USA; Kurt H. Piepenbrink, Department of Food Science and Technology, University of Nebraska—Lincoln, Lincoln, Nebraska, USA; William D. Thomas, Jr., Paragon Bioservices, Baltimore, Maryland, USA.

Hepatitis C virus (HCV) is a major global health concern, infecting 3% of the world's population (1). The majority of those infected progress to chronic HCV infection, which often leads to cirrhosis, liver failure, and hepatocellular carcinoma, a deadly liver cancer (2). Liver transplantation, undertaken for those with cirrhosis and liver cancer, does not eliminate the virus completely, resulting in viral rebound and infection of the transplanted liver (2). Despite advances in treatment methods for HCV, including recently approved direct acting antivirals, high treatment cost and a high rate of asymptomatic and untreated infections make a prophylactic vaccine necessary for global control of HCV (1).

After decades of research, as well as several candidates in phase I and phase II clinical trials (3), no approved HCV vaccine is available. This is in part due to the high diversity of the virus within individuals, arising from error-prone replication and estimated to be 10-fold greater than that of HIV, leading to generation of a number of viral quasispecies that allow it to readily escape from the immune response (4). The identification of broadly neutralizing antibodies (bnAbs) that target conserved and functionally important regions of the E1 and E2 glycoproteins on the viral surface (5), as well as structural characterization of several bnAb-epitope complexes (6–13), provides a major opportunity to design vaccines that induce robust antibody responses to one or more of these epitopes (14). Such structure-based vaccine design approaches have been explored for other viruses, such as HIV (15, 16), influenza virus (17, 18), and respiratory syncytial virus (RSV) (19, 20), with promising results, though in some cases neutralizing antibodies were not successfully induced *in vivo*, possibly due to the epitope's context on the viral surface (15) or immunological variability among animal models (20). In the context of HCV, one candidate for immunogen design is the epitope bound by the bnAb HCV1 (21).

HCV1 was generated by immunization of humanized mice with soluble E2 (21) and targets a continuous epitope on the surface of E2 (residues 412 to 423, referred to as epitope I) which is also recognized by a variety of human (22) and murine (23, 24) monoclonal antibodies (MAbs). Tests of the HCV1 MAb in chimpanzees showed evidence of protection from HCV infection as well as reduction in viral load (25), and in humans, HCV1 treatment resulted in a significant delay in viral rebound, versus that with a placebo, following liver transplantation (26). Structural characterization of the HCV1 MAb in complex with this epitope found that epitope I adopts a β hairpin conformation with a type I′ β turn (6), which was later observed in the structures of MAb AP33 (8) and two other MAbs (9) bound to epitope I. Epitope I is targeted by neutralizing antibodies that block E2 binding to the human CD81 receptor, which is required for cell entry, and is distinguished from other CD81-associated sites on E2 because it is a continuous rather than conformational epitope (27); this is supported by a recent global E2 alanine scanning study that assessed binding determinants using a panel of 16 E2-targeting MAbs (28). Due to this apparent decoupling and lack of dependency on the remainder of E2, epitope I is of particular interest for structure-based immunogen design efforts, as noted by others (14).

Given the low seroreactivity to this epitope in infected humans ($<$2.5% out of 245 patient samples) (29), the lack of initial reported success inducing antibodies in mice using the linear epitope (21), and its observed flexibility, which has been highlighted in several recent structural studies (12, 30), we performed rational engineering to stably present this antibody-bound structure to the immune system and improve the antibody response to this conserved epitope. We also designed a novel protein using the E2 core protein structure (7), generating a bivalent E2 core antigen presenting two copies of epitope I on its surface. After confirming antibody binding of designs, as well as atomic-level structure of a cyclic design bound to the HCV1 MAb, we tested the *in vivo* immunogenicity of these designs to compare their degrees of effectiveness at eliciting antibodies that bind epitope I and tested sera of immunized mice for HCV neutralization of several HCV genotypes.

RESULTS

Scaffold search and design of cyclic antigens. As noted previously (31), epitope I is highly conserved across HCV genotypes (Fig. 1A), and key binding residues for HCV1 (6) are nearly fully conserved (L413, 99.8%; N415, 96.6%; G418, 99.8%; and W420, 99.8%, as determined by comparison of more than 600 E2 sequences downloaded from the Los Alamos National Laboratory HCV database [32]). To identify proteins to present the epitope I structure in its β hairpin conformation and type I′ β turn, we searched a set of approximately 7,600 crystal structures of monomeric proteins downloaded from the Protein Data Bank (PDB) (33) using the FAST structural alignment algorithm (34) for substructures matching epitope I in the HCV1 MAb-epitope I crystal structure (6). All structures including matches identified by FAST (approximately half of the original structures) were screened for match length, backbone root mean square distance (RMSD) to the epitope, protein size, and antibody accessibility. To avoid potentially immunogenic regions in scaffolds that would reduce response to the E2 epitope, we searched in particular for scaffolds of small size that would also accommodate antibody binding to the grafted epitope. We found that several structures corresponding to human α-defensins, which are antimicrobial peptides (approximately 30 amino acids in length) of the innate immune system, were optimal in this regard (Fig. 1B).

With a human α-defensin protein identified as a potential scaffold, we searched a set of all defensin structures for further candidate scaffolds in that family of proteins. This was due to experimentally observed self-association of the α-defensins (despite its monomeric bioassembly in the PDB), which are reported to form symmetric dimers via backbone-mediated interactions between β strands of the monomers (35); based on the location of the dimerization interface (36), HCV1 MAb binding would be blocked were the dimerization to take place in the context of the grafted epitope. We identified another class of defensins, θ-defensins, which feature a β hairpin substructure nearly identical to that of α-defensins yet do not appear to stably self-associate (37). These were not part of the original search set, as all available θ-defensin structures were determined by solution nuclear magnetic resonance (NMR) rather than X-ray crystallography. As with α-defensins, they include three disulfide bonds, yet functional and structural characterization by NMR has shown that only one of the disulfide bonds is needed for structure and antimicrobial function (38). Based on the capability of these small (18-residue) cyclic peptides to form stable β hairpin structures nearly identical to the HCV1-bound epitope structure (Fig. 1C), with an average backbone RMSD among 20 NMR models of 0.9 Å, we generated two cyclic peptide designs (Fig. 1D) comprising minimal scaffolded structures of this epitope.

Design of a bivalent E2-based antigen. While a high-resolution structure of the full E2 glycoprotein has yet to be experimentally described, two crystallographic structures of E2 core are available (7, 39); these correspond to engineered truncated variants of E2 from two genotypes. These structures have a shared globular fold, stabilized by numerous disulfide bonds, and epitope I, located near the N terminus of E2, is fully or mostly absent from both structures. Analysis of these structures revealed a distinctive β hairpin at the same location on their surfaces, consisting of residues 625 to 644 (H77 isolate numbering); in one of the two E2 core structures, this site is directly engaged by an antibody (39). Given its high structural similarity to epitope I (backbone RMSD, 0.8 Å) as well as its surface accessibility, we engineered the E2 glycoprotein to display epitope I at this site, resulting in a bivalent E2-based scaffold with two copies of epitope I on its surface (Fig. 2). This was performed in the context of a truncated E2 construct, where we removed most of hypervariable region 1 (HVR1), given its immunogenicity and capacity to mutate (40), as well as C-terminal residues that were disordered in the E2 core crystal structure. This protein, named Truncation 2 (T2), was tested alongside two control antigens, in addition to $E2_{661}$ (Fig. 2C): Truncation 1 (T1), corresponding to wild-type H77 E2 residues 409 to 645 (without the engineered epitope at amino acids [aa] 629 to 640), and Truncation 3 (T3), with the engineered epitope I at aa 629 to 640 and residues 409 to 423 removed.

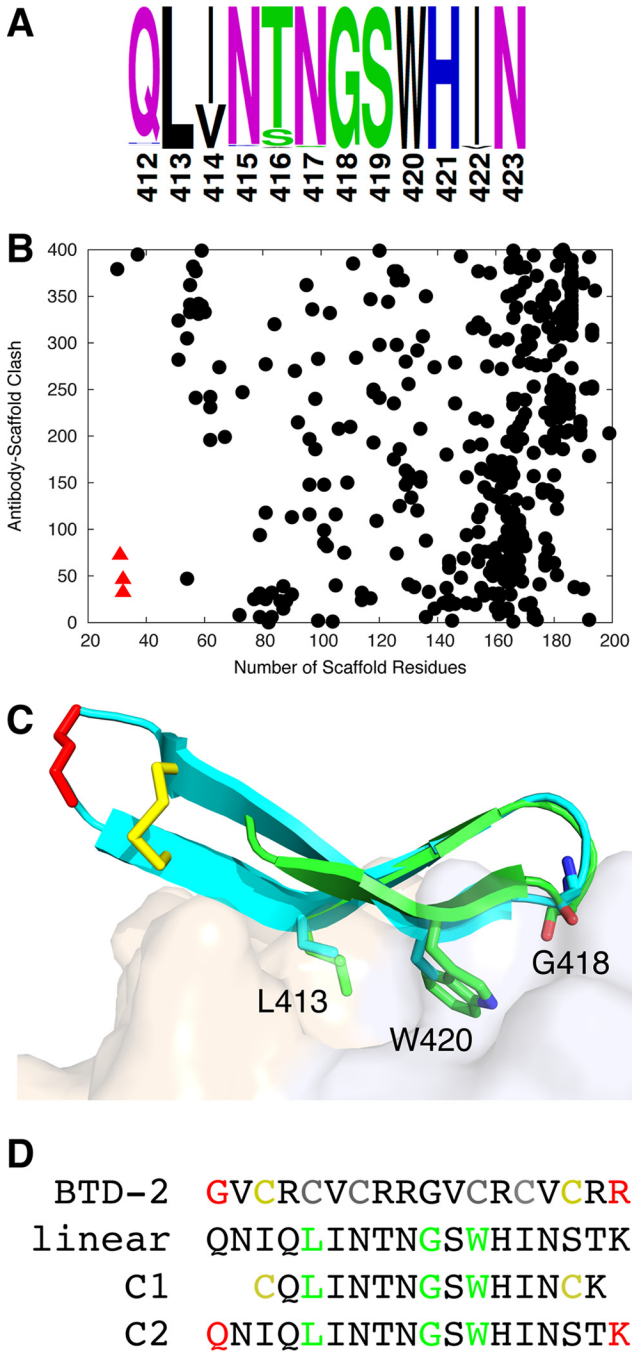

FIG 1 Scaffold search and design of epitope I immunogens. (A) Amino acid residue propensities in epitope I, based on over 600 aligned E2 amino acid sequences downloaded from the Los Alamos National Laboratory HCV database (35) (2008 set). (B) Search of protein crystal structures for epitope I scaffolds. Antibody accessibility (clash of superposed epitope-bound HCV1 antibody structure with scaffold) versus protein size is shown for each candidate scaffold (scaffolds with higher antibody clash are not shown), with three α-defensin structures (PDB codes 1ZMM, 1ZMP, and 1ZMQ) shown as red triangles. (C) Alignment of HCV1-bound E2 epitope I (PDB code 4DGY; green) to an NMR conformer of cyclic θ-defensin (PDB code 2M2S; cyan), which was engineered to remove two out of three internal disulfide bonds; HCV1 MAb (tan and light blue surface for heavy and light chains, respectively) is shown for reference. Backbone root mean square distance (RMSD) between epitope I and matching BTD-2 residues is 0.9 Å. Cyclic residues and those corresponding to key epitope positions L413, G418, and W420 are shown as sticks, with the epitope positions labeled. BTD-2 backbone cyclization is colored red, and disulfide bond is colored yellow. (D) Sequence of BTD-2, and tested linear and cyclic peptides, with cyclized residues colored as in (C), BTD-2 cysteines that were mutated in the NMR structure to remove disulfide bonds colored gray, and positions L413, G418, and W420 colored green. Linear and C2 constructs contain E2 residues 409 to 425, while C1 contains E2 residues 412 to 423; all tested peptides include a C-terminal lysine for carrier protein conjugation.

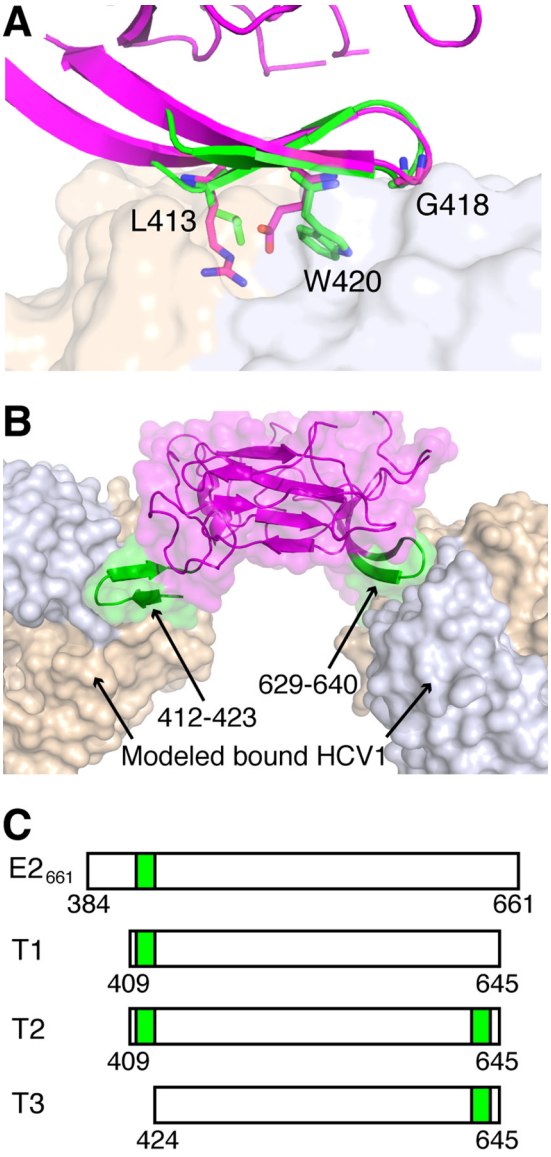

FIG 2 Design of an E2-based epitope I bivalent immunogen. (A) Structure of E2 core (PDB code 4MWF; magenta), aligned to HCV1-bound epitope I (PDB code 4DGY; green) using residues 629 to 640. HCV1 MAb (tan and light blue surface for heavy and light chains, respectively) is shown for reference. Epitope residues L413, G418, and W420, as well as corresponding E2 core residues R630, G635, and E637, are shown as sticks, and epitope positions are labeled. The backbone root mean square distance between epitope I and matching E2 core residues (aa 629 to 640) is 0.8 Å. (B) Model of HCV1 MAb bound to the native epitope I site on E2 (aa 412 to 423) as well as engineered epitope I site at aa 629 to 640, with both sites colored green, and E2 core and MAb colored as in panel A. (C) Tested E2 constructs $E2_{661}$, T1 (truncated native), T2 (truncated bivalent), and T3 (truncated engineered site only), with E2 epitope I sequence locations represented as green boxes.

Antibody binding of designed immunogens. Cyclic epitope I designs were synthesized and tested for binding to the HCV1 MAb using surface plasmon resonance (SPR) (Fig. 3) to confirm epitope integrity in the context of the cyclization. Though antibody immobilization and peptide analyte were tested, this did not produce sufficient binding signals for analysis; therefore, immobilized peptide and HCV1 MAb analyte were used for SPR assays. Both cyclic designs bound HCV1 with measurable affinities, comparable to that of the linear peptide (within experimental uncertainty); thus, cyclization maintained the capability of these immunogens to engage HCV1.

To characterize the epitope presentation of the E2 constructs, $E2_{661}$ and E2 designs were engineered with a 6×His fusion tag, expressed in HEK-293T cells and purified by

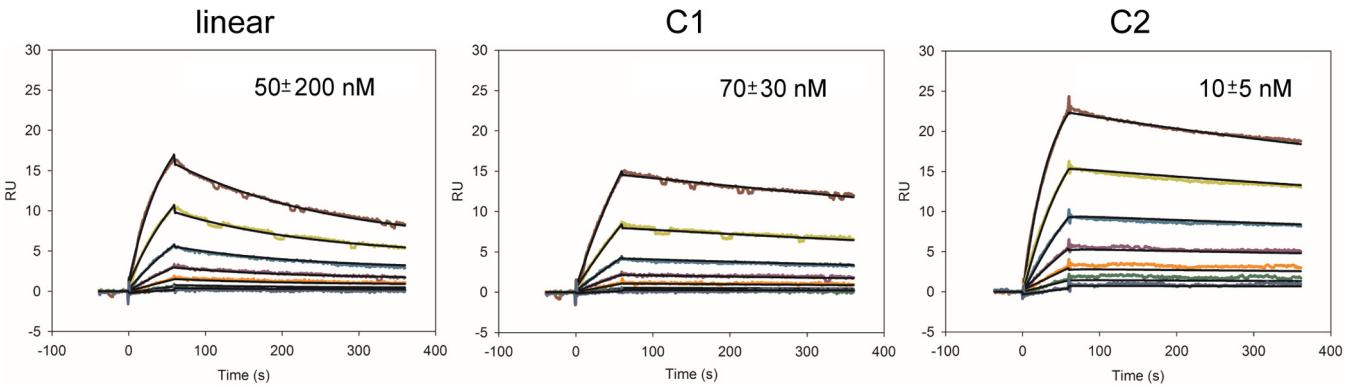

FIG 3 Binding of linear and cyclic peptides to the HCV1 MAb, measured by surface plasmon resonance. Peptides were coupled to bovine serum albumin and immobilized on the chip surface, and binding was measured using a 2-fold dilution series of HCV1 MAb from 125 to 1.9 nM. Fitting of kinetic binding data (black lines) was performed using a bivalent analyte model, and calculated K_{D1} values are shown. K_{D1} represents the initial 2:1 interaction affinity and is calculated as k_{d1}/k_{a1}, where k_{a1} and k_{d1} are the initial interaction association and dissociation rates, respectively. Standard deviations were calculated from four independent experiments.

nickel affinity chromatography. All three truncated E2 designs were expressed at the expected size (Fig. 4). We tested antibody binding in an enzyme-linked immunosorbent assay (ELISA) using HCV1 as well as two other neutralizing antibodies, 95-2 and 96-2 (Fig. 5). Antibody 95-2 is related to HCV1 and binds epitope I (21), while 96-2 binds epitope II (aa 432 to 443) (25); as with HCV1, both were generated using immunization of $E2_{661}$ in mice engineered to express human antibodies (HuMAbs; Medarex, Inc.). All antibodies were engaged by truncated E2 designs T1 to T3, and though there was some (<10-fold) variability in binding to HCV1, binding to 95-2 and 96-2 was more uniform. As no major loss of binding was observed for any of the designed constructs, presentation of epitope I, as well as the epitope II site, was not disrupted in the context of these E2-based designs.

Structural characterization of cyclic C1 immunogen bound to HCV1. To confirm the structure of the designed C1 immunogen, we performed X-ray crystallography to determine its structure in complex with HCV1 (Fig. 6; Table 1). This structure was determined at a resolution of 2.26 Å. A careful comparison of our HCV1-C1 complex structure with the structure of the HCV1 Fab bound to the linear E2 peptide (PDB code 4DGY [6]) revealed preserved binding mode and epitope conformation, as well as densities for the engineered disulfide bond and C-terminal lysine residue (K425) in the C1 peptide. As predicted, we observed no difference in the interface between HCV1 and C1 versus the interface between HCV1 and the linear peptide. We did observe a shift in the conformation of the HCV1 CDR H3 loop in the HCV1-C1 complex crystal structure (Fig. 6G and H), suggesting possible conformational dynamics of that loop; this may additionally be attributed to altered loop context in the crystallographic lattices of these two structures. After superposition of antibody variable (Fv) domains of these complexes, RMSDs between linear and C1 peptides confirm conservation of the epitope structure and binding orientation: 0.37 to 0.48 Å for epitope backbone atoms and 0.83 to 1.09 Å for all epitope atoms (ranges represent values from separate calculations

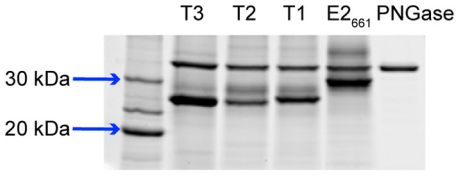

FIG 4 SDS-PAGE gel of purified T1, T2, T3, and $E2_{661}$ proteins. All proteins were treated with peptide-*N*-glycosidase F (PNGase) to remove glycans, which is the upper band (~36 kDa) in each lane (rightmost lane contains PNGase only). Reference sizes are shown on the left. Measured $E2_{661}$ and truncated E2 sizes range from 26 to 31 kDa, corresponding to expected protein sizes.

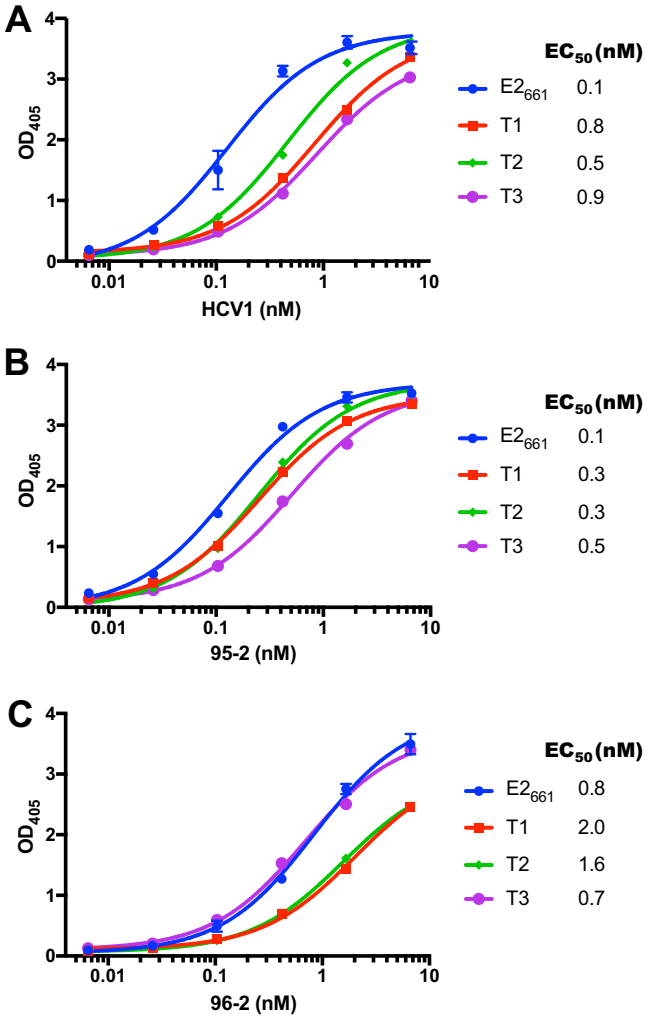

FIG 5 Binding of $E2_{661}$ and designed E2 proteins to neutralizing MAbs HCV1 (A), 95-2 (B), and 96-2 (C) measured by ELISA. Error bars indicate standard deviations from two independent experiments (performed for $E2_{661}$ only), and half-maximal binding titer (EC_{50}) was calculated for each interaction by curve fitting in GraphPad Prism software.

using each of the four asymmetric units of the HCV1-C1 structure), with the larger values for the latter due primarily to Q412, N417, and N423 side chains which are exposed and not directly engaged by the antibody.

Serum antibody response elicited by designed antigens. To compare the antibody responses elicited by engineered epitope I and E2-based antigens, we immunized mice with the two cyclic epitope I peptides and three truncated E2 antigens, alongside control antigens $E2_{661}$ and linear epitope I. Groups of CD1 mice ($n = 4$) were immunized with 50 μg of the peptides or purified E2-based proteins, followed by four 10-μg boosts over approximately 6 weeks. Soluble E2 ($E2_{661}$) was included as a positive control based on its previously described immunogenicity (21). Serum samples were collected 1 week after the fifth immunization, and sera from immunized mice were tested for epitope I-specific antibody response using ELISA (Fig. 7). Mice immunized with the cyclic antigens (C1 and C2) showed strong ELISA reactivity against the epitope I peptide, whereas immunization of the linear peptides resulted in significantly lower serum responses. The $E2_{661}$, T1 (truncated wild-type E2), and T2 (bivalent E2) antigens induced epitope-specific responses comparable to those obtained with the cyclized peptides, with some variability among mice within each group. The T3 antigen, with the native epitope I site removed, induced the lowest epitope-specific responses among

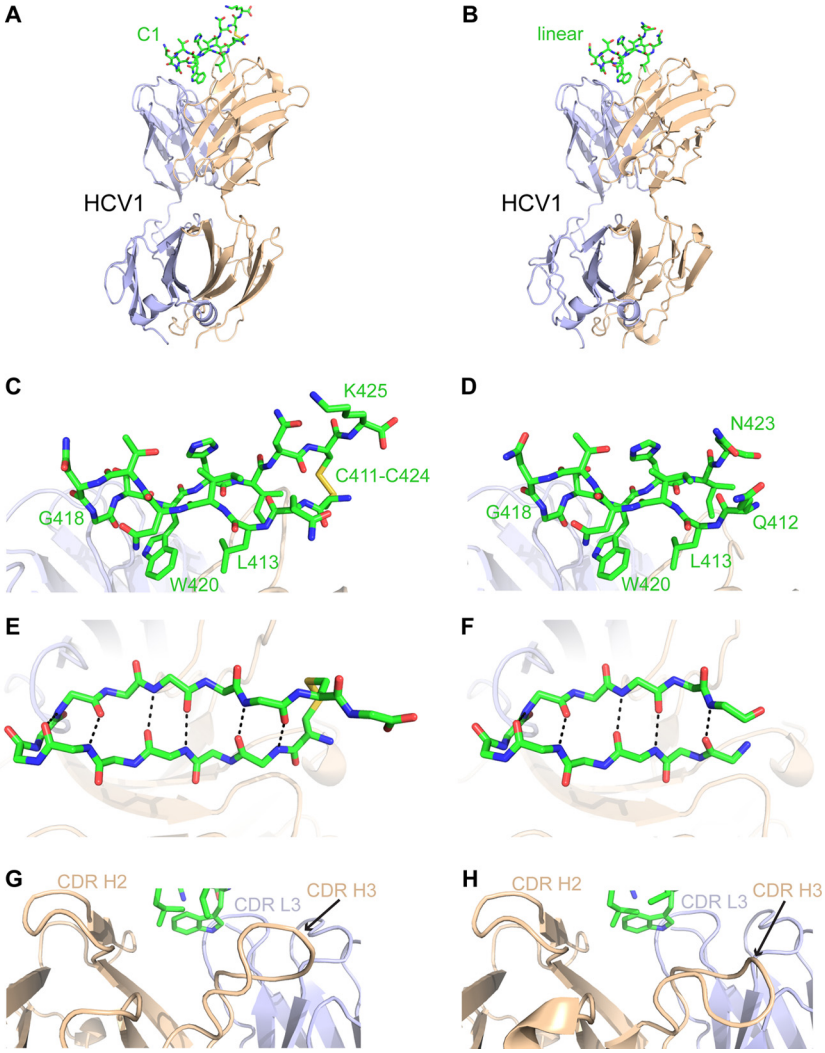

FIG 6 Structure of designed C1 immunogen bound to the HCV1 antibody. The crystallographic structure of full HCV1-C1 complex (A), as well as details of the bound C1 peptide in side view (C), top view (E), and the HCV1 CDR loops (G), are shown in comparison with the structure of the native linear epitope bound to HCV1 (B, D, F, and H), which was previously described (6) (PDB code 4DGY). Peptides are shown as green sticks (with oxygen atoms in red, nitrogen atoms in blue, and sulfur atoms in yellow), and HCV1 antibody is shown as a cartoon with the light chain colored light blue and the heavy chain colored tan. Key epitope residues for HCV1 binding and β turn structure (L413, G418, and W420), as well as terminal and cyclization residues, are labeled in panels C and D, and selected HCV1 CDR loops are labeled in panels G and H. In the top view of the epitope (E and F), side chains are omitted and intrapeptide hydrogen bonds are shown as black dashed lines.

E2-based constructs, indicating that the transplanted epitope at aa 629 to 640 is lower in immunogenicity, or antibodies induced by that site do not cross-react with the native epitope.

Viral neutralization. To determine if the immunized sera could neutralize virus *in vitro*, HCV pseudoparticle (HCVpp) neutralization assays were performed. Mouse sera were tested against HCVpp with H77 E1E2 sequences (Fig. 8; Table 2). Immunization with either cyclic peptide yielded measurable levels of neutralizing antibodies, with some variability within each group. However, no detectable neutralizing antibodies were generated in mice immunized with linear peptides, indicating that the engineered cyclic variants are superior immunogens. Mice immunized with the E2-based antigens showed higher neutralizing antibody responses than the peptide antigens, likely due to the presence of additional epitopes outside epitope I capable of inducing neutralizing antibodies (41, 42), though, as noted by others, at least one such region (corresponding

TABLE 1 X-ray data collection and structure refinement statistics

Parameter	Value(s) for HCV1-C1
Data collection	
Resolution (Å)	29.49–2.26 (2.29–2.26)
Space group	P1
Unit cell	
a, *b*, *c* (Å)	47.07, 94.54, 126.76
α, β, γ (°)	91.84, 94.95, 97.91
No. of reflections	186,455
No. of unique reflections	96,679 (8,406)
Completeness (%)	92.68 (61.00)
R_{merge}[b]	0.069
Refinement	
R_{work} (%)[a,c]	21.81 (30.99)
R_{free} (%)[a,c]	26.09 (34.27)
No. of protein atoms	14,030
No. of water molecules	548
RMSDs from ideality	
Bond length (Å)	0.012
Bond angles (°)	1.59
Ramachandran plot statistics (%)	
Favored	96.1
Allowed	3.6
Forbidden	0.3

[a]Values in parentheses are statistics for the highest-resolution shell.
[b]Rmerge = $\Sigma_h\Sigma_i|I_{hi} - <I_h>|/\Sigma_{h,i}I_{hi}$, where I_{hi} is the *i*th observation of the reflection *h*, while $<I_h>$ is its mean intensity.
[c]$R_{work} = \Sigma||F_o| - |F_c||/\Sigma|F_o|$, where F_c is the calculated structure factor. R_{free} is as for R_{work} but calculated for a randomly selected 5% of reflections not included in the refinement.

to epitope II, which is targeted by the 96-2 MAb) is associated with viral escape (43). Among these antigens, $E2_{661}$ and T1 induced the highest levels of H77 neutralizing antibodies, with T2 and T3 constructs containing the transplanted epitope at aa 629 to 640 yielding lower neutralizing antibody responses.

To assess neutralization breadth, we tested serum neutralization using HCVpps derived from genotype 1b and 4a isolates (Table 2), which were used previously to characterize HCV1 MAb neutralization (21). For all constructs, neutralization activity against these was lower than for H77, suggesting limited neutralization breadth overall. The T1 design maintained the neutralization of the genotype 1b HCVpps with respect to $E2_{661}$, with possible modest improvement. For the designed cyclic constructs,

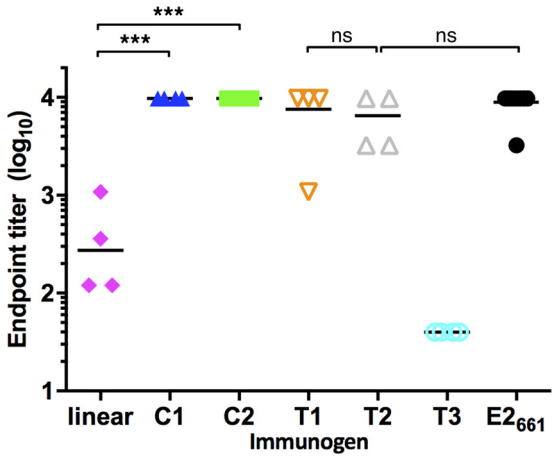

FIG 7 Binding of immunized mouse sera to epitope I. Four mice per group were immunized with E2-based or peptide construct, and sera were tested using ELISA for binding to a linear epitope I peptide (aa 409 to 425, H77 sequence) conjugated to BSA, using a coating concentration of 2 μg/ml. *P* values were calculated using a two-tailed *t* test (***, $P \leq 0.001$; ns, not significant [$P > 0.05$]).

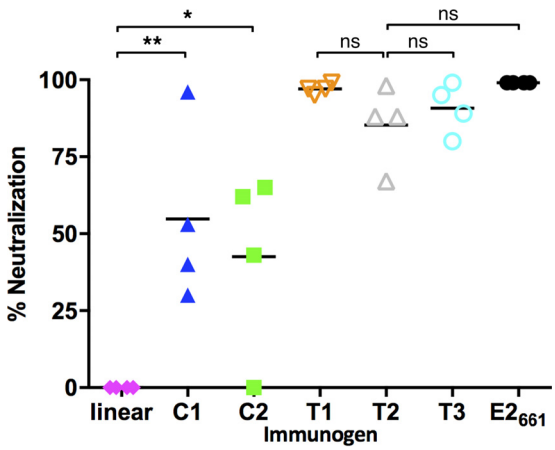

FIG 8 HCV neutralization of immunized mouse sera. Four mice per group were immunized with E2-based or peptide construct, and sera were tested using the HCVpp assay for genotype 1a neutralization. The neutralization activity at a serum dilution of 1:64 was normalized with the activity of preimmune serum and expressed as percentage of neutralization for each animal. Lines indicate mean values for each group. *P* values were calculated using a two-tailed *t* test (*, $P \leq 0.05$; **, $P \leq 0.01$; ns, not significant [$P > 0.05$]).

neutralization breadth was limited, suggesting that despite robust epitope I-specific responses, limited sequence variability within the epitope (I414V for the 1b isolate and T416S for the 4a isolate [21]) or other variations in viral sequence or fitness reduced the neutralization capacity of immunized sera against these isolates.

DISCUSSION

Structure-based HCV vaccine design has seen limited success recently reported by others. One study described structure-based design of scaffolded antigens for HCV to display an E1 epitope as well as E2 epitope I (44). Though the latter constructs were tested for binding to the HCV1 antibody, no *in vivo* results were reported. The designs resulting from the metaserver methodology described in that study were larger and distinct from the cyclic designs we produced and tested *in vivo*. More recently, a study was reported featuring a cyclic epitope I construct with a different mode of disulfide cyclization than C1 or C2, including epitope residues 412 to 422 rather than 412 to 423 (C1) or 409 to 425 (C2) and no glycan at N417 (45). After mouse immunization with this antigen, several elicited MAbs were tested for epitope binding and neutralization, but no measurable neutralization was observed. By employing two distinct design approaches, scaffolding of the epitope to present the stabilized epitope structure to the immune system (C1 and C2), and antigen redesign (T1, T2, and T3), we were able to provide an unprecedented comparison of these widely different design strategies *in vivo* for their potential to elicit epitope-specific and neutralizing antibodies to HCV, along with structural characterization of a designed immunogen.

Although the bivalent E2 construct we produced (T2) yielded lower neutralizing antibody responses than the monovalent control (T1) based on H77 50% neutralization (ID_{50}) values (Table 2), further exploration of this approach may be warranted. One advantage of this bivalent antigen not considered in the design strategy was the disruption via mutation of an E2 epitope associated with nonneutralizing antibodies that includes residue Y632 (28). Furthermore, the absence of HVR1 in T2 and other truncated constructs is an advantage over $E2_{661}$, as that region is associated with high sequence variability and escape from neutralizing antibodies (40). However, its reduced capacity to induce neutralizing antibodies, and the lack of apparent improvement in levels of epitope I-specific antibodies, suggests that the T2 antigen requires further design to improve presentation of the transplanted epitope, and possibly its stability. One option in this regard would be design to optimize the E2 core-epitope interface at aa 629 to 640, which was not performed originally in order to preserve the full epitope

TABLE 2 Serum neutralization in immunized mice[a]

Immunogen	Mouse no.	% Neutralization			H77 ID_{50}
		H77 (1a)	1b	4a	
Linear	1	0			<64
	2	0			<64
	3	0			<64
	4	0			<64
C1	1	96	0	0	720
	2	40	23	0	<64
	3	30	0	0	<64
	4	53	0	0	<64
C2	1	62	20	4	70
	2	0	0	0	<64
	3	43	23	0	<64
	4	65	37	0	110
T1	1	97	64	0	>5,000
	2	99	92	18	>5,000
	3	97	0	0	890
	4	95	91	20	870
T2	1	88	0	18	100
	2	88	15	24	190
	3	98	87	0	>5,000
	4	67	0	8	<64
T3	1	95	33	16	425
	2	99	27	19	>5,000
	3	80	28	15	75
	4	89	23	45	400
$E2_{661}$	1	99	10	0	>5,000
	2	99	10	23	3,470
	3	99	70	0	>5,000
	4	99	10	28	>5,000

[a]Percent neutralization was measured using HCV pseudoparticle (HCVpp) assays and is shown for a serum dilution of 1:64, with HCVpp representing genotypes 1a (isolate H77), 1b (isolate 1b-#2), and 4a (isolate 4a-MJ). Dilution levels corresponding to 50% neutralization (ID_{50}) were calculated for H77 by curve fitting in GraphPad Prism software. Shading indicates >50% neutralization at the 1:64 dilution or an H77 ID_{50} of ≥100. Due to low H77 neutralization, genotype 1b and 4a HCVpp neutralization of linear peptide-immunized mice was not tested.

sequence. Such designs could include removal of the glycan at epitope position N417 via mutation of N417 or S419, in conjunction with other substitutions of non-HCV1 contact residues proximal to E2 core to improve packing and shape complementarity. Intriguingly, others have recently noted that for another truncated variant of E2 (with HVR1 to HVR3 removed), high-molecular-weight forms of the protein improve neutralizing antibody responses, thus providing an additional route to increase the neutralization potency and breadth of these E2-based designs (46). While we did observe epitope I-specific and neutralizing antibodies elicited by our truncated designs, epitope II and other sites on E2 may indeed be targeted by the neutralizing response; the extent of epitope I-specific neutralizing antibodies can possibly be probed in future work through additional assays, such as inhibition of HCVpp neutralization using epitope I peptide.

The cyclic antigens we generated highlight the potential of minimal stabilized antigens to induce neutralizing epitope-specific antibodies that improve over immunization with the linear peptide. The improvement in immunogenicity does not seem to be due to improved HCV1 binding affinity, as based on our assays there was no significant change, though other binding assays such as isothermal titration calorimetry may help to confirm this. As at least one extended epitope I structure is associated with an antibody with relatively weak neutralization (12), and cyclization would avoid or

disfavor such a conformation, it is possible that constraining the epitope conformation could affect the quality of the antibody response. However, given the improvement in epitope-specific antibody titers from cyclic designs, other factors, such as improved serum stability and half-life of the cyclic designs, may be responsible. Though the levels of neutralizing antibodies induced by the cyclic epitopes were relatively low, compared with those obtained with sera from $E2_{661}$-immunized animals, and exhibited limited neutralization breadth, a number of options are available to improve neutralizing antibody response, including display of the cyclic immunogens on virus-like particles or nanoparticles (47). Heterologous prime-boost vaccination, with E2 or E1E2 protein as the prime followed by boost with cyclic epitope I to focus the response to that portion of E2, as utilized by others for HIV vaccination (48), may also improve levels of epitope I-specific neutralizing antibodies.

The limited neutralization breadth elicited by the cyclic constructs is possibly related to recent observations of HCV neutralization where certain isolates exhibit broad nAb resistance, which was correlated with overall viral infectivity for a large panel of HCVpps (49). In another study, non-epitope E2 residues affecting coreceptor binding appeared to be responsible for resistance (50), while others have noted variability in neutralization with MAbs targeting epitope I, despite conserved epitope sequence (22). A deep-sequencing analysis including patients undergoing HCV1 MAb immunotherapy revealed E1 and E2 positions outside epitope I with relatively high mutation rates, suggesting a possible direct or indirect role in evading antibody targeting of that epitope (51). In light of the relatively low but detectable levels of H77 neutralization, it is possible that even modest (2- to 4-fold) increases in resistance in the 1b and 4a HCVpps tested led to a lack of measurable neutralization by the sera from animals immunized with cyclic peptides, and modifications in immunogen display as noted above would lead to more detectable and robust neutralization breadth. HCVpps representing a larger set of isolates can be included in follow-up studies of these designs to provide more support of neutralization breadth or lack thereof.

Further design of the cyclic constructs may also yield improved responses. Characterization of MAbs induced by C1 or C2 vaccination, via alanine scanning mutagenesis, affinity measurements, or crystallography, may yield information regarding the induced repertoire and possible molecular details underlying the observed difference between epitope I-specific binding and neutralization, for instance, MAb binding to portions of the epitope that are inaccessible in the context of E2 or the virion. Such characterization of C1 and C2-elicited MAbs, which was utilized recently for another cyclic epitope I design as noted above (45), could indicate the basis of neutralization in immunized sera from our constructs and inform second-generation designs of one or both of those antigens. Additionally, as glycosylation or mutation at N415 is associated with escape from HCV1 (25, 51) and other MAbs (9), addition of a glycan at N415, in addition to N417, may induce antibodies capable of targeting this epitope with a binding footprint that does not include N415 while maintaining binding to the conserved residues L413 and W420. Given the glycan sequons of NxT and NxS, simultaneous glycosylation at N415 and N417 is possible only in a synthetic peptide (such as the ones described here) rather than an expressed protein antigen. Recently described structural characterization of an epitope I-targeting MAb, HC33.1, that can neutralize the glycan-shifted N417S variant and engages the epitope in a unique extended conformation may lead to additional scaffolded or stabilized designed antigens (30). We have shown in this study, using the HCV1-bound epitope I conformation, that such an approach is possible and merits further investigation.

MATERIALS AND METHODS

Scaffold selection. A set of 7,626 potential scaffold structures was downloaded from the Protein Data Bank (PDB) (33) in February 2013. All structures were monomeric (one protein chain in the biological assembly), expressed in *Escherichia coli*, and determined by X-ray crystallography and contained fewer than 200 residues. The structural alignment program FAST (34) was used to identify any structurally similar region to epitope I (PDB code 4DGY, chain A) within each structure. Approximately half of the structures (4,200) contained regions identified by FAST as structurally similar to the epitope; these results

were analyzed to determine length of match, root mean square distance (RMSD) to the epitope (both computed by FAST), and accessibility for antibody binding. The last value was determined by counting the atomic contacts (<4.0 Å) between the HCV1 MAb and scaffold (excluding the epitope-matching residues) after superposing the scaffold onto the epitope in the HCV1-epitope complex structure using FAST.

Protein expression and purification. The nucleic acid sequences encoding HCV E2 (genotype 1a isolate H77; GenBank accession number NC004102) aa 384 to 661 (referred to as $E2_{661}$) and its designed truncated constructs (T1, T2, and T3) were synthesized and cloned into a mammalian expression vector, pcDNA3.1 (Life Technologies), in frame with an N-terminal histidine (His) tag. Cloned vectors were transfected into HEK-293T cells using Lipofectamine 2000 (Life Technologies) as described by the manufacturer. Cells were grown to confluence in T150 flasks in 15 ml of Dulbecco modified Eagle medium (DMEM) with 10% fetal bovine serum (FBS). Thirty micrograms of DNA was mixed with 75 μl of Lipofectamine 2000, and the mixture was added to the cells for overnight incubation at 37°C. Medium was removed 24 h posttransfection and replaced with fresh complete DMEM. A 3 mM concentration of sodium butyrate (Sigma-Aldrich) was added to the medium 48 h posttransfection, and the supernatants were harvested after an additional 24-h incubation. Filtered supernatants were mixed with nickel-nitrilotriacetic acid (Ni-NTA) agarose (Life Technologies) for 2 h at room temperature, and proteins were eluted with 250 mM imidazole (Sigma-Aldrich). Eluted proteins were dialyzed against phosphate-buffered saline (PBS), concentrated, and stored in single-use aliquots at −80°C. Protein integrity and purity were evaluated by SDS-PAGE with Coomassie staining and by Western blotting using mouse anti-His antibody.

Peptides. Linear and cyclized peptides including the H77 epitope I sequence (QNIQLINTNGSWHI NSTK and CQLINTNGSWHINCK) were produced at New England Peptide (Gardner, MA), conjugated to bovine serum albumin (BSA) or keyhole limpet hemocyanin (KLH) carrier protein via glutaraldehyde at the C-terminal lysine side chain. For peptides without backbone cyclization, N termini were modified via acetylation to improve coupling and prevent N-terminal glutamine conversion to pyroglutamic acid (in the case of linear peptide). Peptides produced for immunogenicity studies were N-glycosylated at the position corresponding to N417 with the *N*-acetylglucosamine (GlcNAc) glycan.

ELISA. Ninety-six-well plates were coated with antigens (peptide, $E2_{661}$, or E2 truncations) at a concentration of 2 μg/ml, followed by incubation overnight at 4°C. Mouse serum or purified antibody was added to the 96-well plates and incubated for 1 h at room temperature. Antibody binding was detected with anti-human alkaline phosphatase secondary antibody and *p*-nitrophenyl phosphate disodium salt (PNPP) substrate.

SPR. All surface plasmon resonance (SPR) experiments were performed using a Biacore T100 instrument (GE Healthcare). Soluble BSA (New England BioLabs), C2 peptide-BSA, C1 peptide-BSA, and the linear peptide-BSA in 10 mM sodium acetate, pH 4.0, were immobilized on a CM5 sensor chip via a standard amine coupling procedure at densities of 1,322 response units (RU) to flow cell 1, 796 RU to flow cell 2, 124 RU to flow cell 3, and 101 RU to flow cell 4, respectively. HBS-X buffer (10 mM HEPES, 150 mM NaCl, 0.05% Tween) was used as a running buffer. BSA coupled to the sensor chip in flow cell 1 was used as the negative-control surface. A concentration series of HCV1 MAbs (125 to 1.9 nM) in running buffer was injected over flow cells 1 to 4 for 60 s per injection and allowed to dissociate for 300 s. Between binding cycles, the sensor chip surface was regenerated by washing with 2 M NaCl. Kinetic parameters and affinity constants for all interactions were calculated using a kinetic model for bivalent analytes (as HCV1 was in IgG rather than Fab format) with Biacore T100 evaluation software 2.0.4.

X-ray crystallography. HCV1 Fab was separated from the Fc by papain using standard protocols, purified by size exclusion chromatography on a GE Superdex S200, concentrated to 10 mg/ml in 20 mM Tris–100 mM NaCl (pH 8.3), and incubated with a 10-fold excess of the C1 peptide (CQLINTNGSWHINCK). Crystals formed after 1 week by vapor diffusion in 0.2 M calcium acetate, 0.1 M morpholineethanesulfonic acid (MES; pH 6.0), and 20% polyethylene glycol 4000 (PEG 4000) at a drop ratio of 1:1. Glycerol was added at 20% as a cryoprotectant, and data were collected at the Stanford Synchrotron Radiation Lightsource, beamline 9-2, and the Advanced Photon Source, beamline 23-ID-D. The data were integrated by XDS at a 2.26-Å resolution, phased using molecular replacement by Phaser, built using Coot, and refined by Phenix refine and Refmac (52–55).

Modeling of HCV1 MAb bound to E2. Modeling of HCV1 MAb bound to E2 at residues 412 to 423 was performed by aligning the HCV1-epitope I complex (PDB code 4DGY) onto the E2 core structure (PDB code 4MWF, chain D) using root mean square fitting of the backbone atoms of shared E2 residue N423. The FloppyTail algorithm in Rosetta (56) was then used to perform minimization of HCV1-epitope I in the context of E2 core, to reduce clash between HCV1 and E2 core, treating the backbone of residue 423 as a flexible hinge. One hundred models were generated, of which the top model was selected based on Rosetta score and paucity of MAb contacts with E2 core (as HCV1 targets a linear epitope, extensive contacts with E2 core are not likely, as supported by a global alanine scanning study with other antibodies targeting epitope I [28]). HCV1 was fit by backbone superposition of epitope I residues onto residues 629 to 640 of E2 core to model its engagement of the transplanted epitope.

***In vivo* studies.** CD-1 mice (Charles River) were injected intraperitoneally with purified protein mixed with Sigma Adjuvant System (SAS) adjuvant (Sigma-Aldrich) with 50 μg of prime immunization and four 10-μg boosts given weekly, except for a gap of 2 to 3 weeks between the second and third boosts. Animals were sacrificed approximately 10 days after final injection, and sera were collected for neutralization and binding assays.

HCV transfection, infection, and neutralization assays. Pseudovirus was generated by using a replication-defective HIV backbone containing a firefly luciferase gene to direct luciferase expression in

target cells (pNL4-3.Luc.R−E−, obtained through the AIDS Research and Reference Program, Division of AIDS, NIAID, NIH, from Nathaniel Landau). The nucleic acid sequences encoding HCV E1E2 glycoprotein from isolates H77 (genotype 1a), 1b-#2 (genotype 1b), and 4a-MJ (genotype 4a), GenBank accession numbers NC_004102, GQ259488, and GQ379230, respectively, were cloned into pcDNA3.1 vector as described previously (21). The pcDNA-E1E2 vectors were cotransfected with pNL4-3.Luc.R−E− into HEK-293T cells using Lipofectamine 2000 (Life Technologies). Pseudoviral particles were harvested 48 to 72 h posttransfection, concentrated using a Centricon 70 concentrator (Millipore), aliquoted, and stored frozen at 80°C. Before assessing antibody neutralization, a titration of HCVpps was performed on Hep3B cells to determine what volume of virus generated 50,000 cps in the infection assay. The appropriate volume of HCVpps was preincubated with various dilutions of mouse serum or HCV1 for 1 h at room temperature before addition to Hep3B cells. After incubation for 72 h (31), infection was quantified by luciferase detection (Bright-Glo reagent; Promega) and read in a Victor 3 plate reader (PerkinElmer) for light production.

Figures. Figures showing molecular structures were generated using PyMOL (Schrodinger, LLC), and plots of ELISA and neutralization data were generated using GraphPad Prism. The epitope I sequence logo was generated using the WebLogo program (32).

Accession number(s). The structure of the designed C1 immunogen in complex with the HCV1 MAb has been deposited in the PDB under accession code 5KZP.

ACKNOWLEDGMENTS

Research reported in this publication was supported by the National Center for Advancing Translational Sciences of the NIH under award number UL1-TR001453. B.G.P. was additionally supported through startup funding from the University of Maryland and NIH grant R21-AI126582.

The content is solely the responsibility of the authors and does not necessarily represent the official views of the NIH.

We thank Gregory J. Babcock for helping to initiate this project and Mark S. Klempner for useful suggestions on study design, as well as Steven K. H. Foung and Zhenyong Keck (Stanford University School of Medicine) for their comments on the manuscript. We additionally thank Bob Beadenkopf for outstanding technical assistance and the beamline support staff at Stanford Synchrotron Radiation Lightsource and Advanced Photon Source.

REFERENCES

1. Cox AL. 2015. Global control of hepatitis C virus. Science 349:790–791. https://doi.org/10.1126/science.aad1302.
2. Lauer GM, Walker BD. 2001. Hepatitis C virus infection. N Engl J Med 345:41–52. https://doi.org/10.1056/NEJM200107053450107.
3. Dunlop J, Owsianka A, Cowton V, Patel A. 2015. Current and future prophylactic vaccines for hepatitis C virus. Vaccine Dev Ther 2015:31–44.
4. Halliday J, Klenerman P, Barnes E. 2011. Vaccination for hepatitis C virus: closing in on an evasive target. Expert Rev Vaccines 10:659–672. https://doi.org/10.1586/erv.11.55.
5. Cashman SB, Marsden BD, Dustin LB. 2014. The humoral immune response to HCV: understanding is key to vaccine development. Front Immunol 5:550. https://doi.org/10.3389/fimmu.2014.00550.
6. Kong L, Giang E, Robbins JB, Stanfield RL, Burton DR, Wilson IA, Law M. 2012. Structural basis of hepatitis C virus neutralization by broadly neutralizing antibody HCV1. Proc Natl Acad Sci U S A 109:9499–9504. https://doi.org/10.1073/pnas.1202924109.
7. Kong L, Giang E, Nieusma T, Kadam RU, Cogburn KE, Hua Y, Dai X, Stanfield RL, Burton DR, Ward AB, Wilson IA, Law M. 2013. Hepatitis C virus E2 envelope glycoprotein core structure. Science 342:1090–1094. https://doi.org/10.1126/science.1243876.
8. Kong L, Giang E, Nieusma T, Robbins JB, Deller MC, Stanfield RL, Wilson IA, Law M. 2012. Structure of hepatitis C virus envelope glycoprotein E2 antigenic site 412 to 423 in complex with antibody AP33. J Virol 86:13085–13088. https://doi.org/10.1128/JVI.01939-12.
9. Pantua H, Diao J, Ultsch M, Hazen M, Mathieu M, McCutcheon K, Takeda K, Date S, Cheung TK, Phung Q, Hass P, Arnott D, Hongo JA, Matthews DJ, Brown A, Patel AH, Kelley RF, Eigenbrot C, Kapadia SB. 2013. Glycan shifting on hepatitis C virus (HCV) E2 glycoprotein is a mechanism for escape from broadly neutralizing antibodies. J Mol Biol 425:1899–1914. https://doi.org/10.1016/j.jmb.2013.02.025.
10. Deng L, Zhong L, Struble E, Duan H, Ma L, Harman C, Yan H, Virata-Theimer ML, Zhao Z, Feinstone S, Alter H, Zhang P. 2013. Structural evidence for a bifurcated mode of action in the antibody-mediated neutralization of hepatitis C virus. Proc Natl Acad Sci U S A 110:7418–7422. https://doi.org/10.1073/pnas.1305306110.
11. Krey T, Meola A, Keck ZY, Damier-Piolle L, Foung SK, Rey FA. 2013. Structural basis of HCV neutralization by human monoclonal antibodies resistant to viral neutralization escape. PLoS Pathog 9:e1003364. https://doi.org/10.1371/journal.ppat.1003364.
12. Meola A, Tarr AW, England P, Meredith LW, McClure CP, Foung SK, McKeating JA, Ball JK, Rey FA, Krey T. 2015. Structural flexibility of a conserved antigenic region in hepatitis C virus glycoprotein E2 recognized by broadly neutralizing antibodies. J Virol 89:2170–2181. https://doi.org/10.1128/JVI.02190-14.
13. Kong L, Kadam RU, Giang E, Ruwona TB, Nieusma T, Culhane JC, Stanfield RL, Dawson PE, Wilson IA, Law M. 2015. Structure of hepatitis C virus envelope glycoprotein E1 antigenic site 314-324 in complex with antibody IGH526. J Mol Biol 427:2617–2628. https://doi.org/10.1016/j.jmb.2015.06.012.
14. Kong L, Jackson KN, Wilson IA, Law M. 2015. Capitalizing on knowledge of hepatitis C virus neutralizing epitopes for rational vaccine design. Curr Opin Virol 11:148–157. https://doi.org/10.1016/j.coviro.2015.04.001.
15. Ofek G, Guenaga FJ, Schief WR, Skinner J, Baker D, Wyatt R, Kwong PD. 2010. Elicitation of structure-specific antibodies by epitope scaffolds. Proc Natl Acad Sci U S A 107:17880–17887. https://doi.org/10.1073/pnas.1004728107.
16. Jardine J, Julien JP, Menis S, Ota T, Kalyuzhniy O, McGuire A, Sok D, Huang PS, MacPherson S, Jones M, Nieusma T, Mathison J, Baker D, Ward AB, Burton DR, Stamatatos L, Nemazee D, Wilson IA, Schief WR. 2013. Rational HIV immunogen design to target specific germline B cell receptors. Science 340:711–716. https://doi.org/10.1126/science.1234150.
17. Yassine HM, Boyington JC, McTamney PM, Wei CJ, Kanekiyo M, Kong WP, Gallagher JR, Wang L, Zhang Y, Joyce MG, Lingwood D, Moin SM, Andersen H, Okuno Y, Rao SS, Harris AK, Kwong PD, Mascola JR, Nabel GJ, Graham BS. 2015. Hemagglutinin-stem nanoparticles generate het-

erosubtypic influenza protection. Nat Med 21:1065–1070. https://doi.org/10.1038/nm.3927.
18. Impagliazzo A, Milder F, Kuipers H, Wagner MV, Zhu X, Hoffman RM, van Meersbergen R, Huizingh J, Wanningen P, Verspuij J, de Man M, Ding Z, Apetri A, Kukrer B, Sneekes-Vriese E, Tomkiewicz D, Laursen NS, Lee PS, Zakrzewska A, Dekking L, Tolboom J, Tettero L, van Meerten S, Yu W, Koudstaal W, Goudsmit J, Ward AB, Meijberg W, Wilson IA, Radosevic K. 2015. A stable trimeric influenza hemagglutinin stem as a broadly protective immunogen. Science 349:1301–1306. https://doi.org/10.1126/science.aac7263.
19. McLellan JS, Chen M, Joyce MG, Sastry M, Stewart-Jones GB, Yang Y, Zhang B, Chen L, Srivatsan S, Zheng A, Zhou T, Graepel KW, Kumar A, Moin S, Boyington JC, Chuang GY, Soto C, Baxa U, Bakker AQ, Spits H, Beaumont T, Zheng Z, Xia N, Ko SY, Todd JP, Rao S, Graham BS, Kwong PD. 2013. Structure-based design of a fusion glycoprotein vaccine for respiratory syncytial virus. Science 342:592–598. https://doi.org/10.1126/science.1243283.
20. Correia BE, Bates JT, Loomis RJ, Baneyx G, Carrico C, Jardine JG, Rupert P, Correnti C, Kalyuzhniy O, Vittal V, Connell MJ, Stevens E, Schroeter A, Chen M, Macpherson S, Serra AM, Adachi Y, Holmes MA, Li Y, Klevit RE, Graham BS, Wyatt RT, Baker D, Strong RK, Crowe JE, Jr, Johnson PR, Schief WR. 2014. Proof of principle for epitope-focused vaccine design. Nature 507:201–206. https://doi.org/10.1038/nature12966.
21. Broering TJ, Garrity KA, Boatright NK, Sloan SE, Sandor F, Thomas WD, Jr, Szabo G, Finberg RW, Ambrosino DM, Babcock GJ. 2009. Identification and characterization of broadly neutralizing human monoclonal antibodies directed against the E2 envelope glycoprotein of hepatitis C virus. J Virol 83:12473–12482. https://doi.org/10.1128/JVI.01138-09.
22. Keck Z, Wang W, Wang Y, Lau P, Carlsen TH, Prentoe J, Xia J, Patel AH, Bukh J, Foung SK. 2013. Cooperativity in virus neutralization by human monoclonal antibodies to two adjacent regions located at the amino terminus of hepatitis C virus E2 glycoprotein. J Virol 87:37–51. https://doi.org/10.1128/JVI.01941-12.
23. Tarr AW, Owsianka AM, Timms JM, McClure CP, Brown RJ, Hickling TP, Pietschmann T, Bartenschlager R, Patel AH, Ball JK. 2006. Characterization of the hepatitis C virus E2 epitope defined by the broadly neutralizing monoclonal antibody AP33. Hepatology 43:592–601. https://doi.org/10.1002/hep.21088.
24. Sabo MC, Luca VC, Prentoe J, Hopcraft SE, Blight KJ, Yi M, Lemon SM, Ball JK, Bukh J, Evans MJ, Fremont DH, Diamond MS. 2011. Neutralizing monoclonal antibodies against hepatitis C virus E2 protein bind discontinuous epitopes and inhibit infection at a postattachment step. J Virol 85:7005–7019. https://doi.org/10.1128/JVI.00586-11.
25. Morin TJ, Broering TJ, Leav BA, Blair BM, Rowley KJ, Boucher EN, Wang Y, Cheslock PS, Knauber M, Olsen DB, Ludmerer SW, Szabo G, Finberg RW, Purcell RH, Lanford RE, Ambrosino DM, Molrine DC, Babcock GJ. 2012. Human monoclonal antibody HCV1 effectively prevents and treats HCV infection in chimpanzees. PLoS Pathog 8:e1002895. https://doi.org/10.1371/journal.ppat.1002895.
26. Chung RT, Gordon FD, Curry MP, Schiano TD, Emre S, Corey K, Markmann JF, Hertl M, Pomposelli JJ, Pomfret EA, Florman S, Schilsky M, Broering TJ, Finberg RW, Szabo G, Zamore PD, Khettry U, Babcock GJ, Ambrosino DM, Leav B, Leney M, Smith HL, Molrine DC. 2013. Human monoclonal antibody MBL-HCV1 delays HCV viral rebound following liver transplantation: a randomized controlled study. Am J Transplant 13:1047–1054. https://doi.org/10.1111/ajt.12083.
27. Ball JK, Tarr AW, McKeating JA. 2014. The past, present and future of neutralizing antibodies for hepatitis C virus. Antiviral Res 105:100–111. https://doi.org/10.1016/j.antiviral.2014.02.013.
28. Pierce BG, Keck ZY, Lau P, Fauvelle C, Gowthaman R, Baumert TF, Fuerst TR, Mariuzza RA, Foung SK. 26 October 2016. Global mapping of antibody recognition of the hepatitis C virus E2 glycoprotein: implications for vaccine design. Proc Natl Acad Sci U S A https://doi.org/10.1073/pnas.1614942113.
29. Tarr AW, Owsianka AM, Jayaraj D, Brown RJ, Hickling TP, Irving WL, Patel AH, Ball JK. 2007. Determination of the human antibody response to the epitope defined by the hepatitis C virus-neutralizing monoclonal antibody AP33. J Gen Virol 88:2991–3001. https://doi.org/10.1099/vir.0.83065-0.
30. Li Y, Pierce BG, Wang Q, Keck ZY, Fuerst TR, Foung SK, Mariuzza RA. 2015. Structural basis for penetration of the glycan shield of hepatitis C virus E2 glycoprotein by a broadly neutralizing human antibody. J Biol Chem 290:10117–10125. https://doi.org/10.1074/jbc.M115.643528.
31. Owsianka A, Tarr AW, Juttla VS, Lavillette D, Bartosch B, Cosset FL, Ball JK, Patel AH. 2005. Monoclonal antibody AP33 defines a broadly neutralizing epitope on the hepatitis C virus E2 envelope glycoprotein. J Virol 79:11095–11104. https://doi.org/10.1128/JVI.79.17.11095-11104.2005.
32. Kuiken C, Yusim K, Boykin L, Richardson R. 2005. The Los Alamos hepatitis C sequence database. Bioinformatics 21:379–384. https://doi.org/10.1093/bioinformatics/bth485.
33. Berman HM, Westbrook J, Feng Z, Gilliland G, Bhat TN, Weissig H, Shindyalov IN, Bourne PE. 2000. The Protein Data Bank. Nucleic Acids Res 28:235–242. https://doi.org/10.1093/nar/28.1.235.
34. Zhu J, Weng Z. 2005. FAST: a novel protein structure alignment algorithm. Proteins 58:618–627. https://doi.org/10.1002/prot.20331.
35. Pazgier M, Wei G, Ericksen B, Jung G, Wu Z, de Leeuw E, Yuan W, Szmacinski H, Lu WY, Lubkowski J, Lehrer RI, Lu W. 2012. Sometimes it takes two to tango: contributions of dimerization to functions of human alpha-defensin HNP1 peptide. J Biol Chem 287:8944–8953. https://doi.org/10.1074/jbc.M111.332205.
36. Wei G, de Leeuw E, Pazgier M, Yuan W, Zou G, Wang J, Ericksen B, Lu WY, Lehrer RI, Lu W. 2009. Through the looking glass, mechanistic insights from enantiomeric human defensins. J Biol Chem 284:29180–29192. https://doi.org/10.1074/jbc.M109.018085.
37. Conibear AC, Rosengren KJ, Harvey PJ, Craik DJ. 2012. Structural characterization of the cyclic cystine ladder motif of theta-defensins. Biochemistry 51:9718–9726. https://doi.org/10.1021/bi301363a.
38. Conibear AC, Rosengren KJ, Daly NL, Henriques ST, Craik DJ. 2013. The cyclic cystine ladder in theta-defensins is important for structure and stability, but not antibacterial activity. J Biol Chem 288:10830–10840. https://doi.org/10.1074/jbc.M113.451047.
39. Khan AG, Whidby J, Miller MT, Scarborough H, Zatorski AV, Cygan A, Price AA, Yost SA, Bohannon CD, Jacob J, Grakoui A, Marcotrigiano J. 2014. Structure of the core ectodomain of the hepatitis C virus envelope glycoprotein 2. Nature 509:381–384. https://doi.org/10.1038/nature13117.
40. Pierce BG, Keck ZY, Foung SK. 2016. Viral evasion and challenges of hepatitis C virus vaccine development. Curr Opin Virol 20:55–63. https://doi.org/10.1016/j.coviro.2016.09.004.
41. Keck ZY, Li TK, Xia J, Gal-Tanamy M, Olson O, Li SH, Patel AH, Ball JK, Lemon SM, Foung SK. 2008. Definition of a conserved immunodominant domain on hepatitis C virus E2 glycoprotein by neutralizing human monoclonal antibodies. J Virol 82:6061–6066. https://doi.org/10.1128/JVI.02475-07.
42. Keck ZY, Xia J, Wang Y, Wang W, Krey T, Prentoe J, Carlsen T, Li AY, Patel AH, Lemon SM, Bukh J, Rey FA, Foung SK. 2012. Human monoclonal antibodies to a novel cluster of conformational epitopes on HCV E2 with resistance to neutralization escape in a genotype 2a isolate. PLoS Pathog 8:e1002653. https://doi.org/10.1371/journal.ppat.1002653.
43. Keck ZY, Saha A, Xia J, Wang Y, Lau P, Krey T, Rey FA, Foung SK. 2011. Mapping a region of hepatitis C virus E2 that is responsible for escape from neutralizing antibodies and a core CD81-binding region that does not tolerate neutralization escape mutations. J Virol 85:10451–10463. https://doi.org/10.1128/JVI.05259-11.
44. He L, Cheng Y, Kong L, Azadnia P, Giang E, Kim J, Wood MR, Wilson IA, Law M, Zhu J. 2015. Approaching rational epitope vaccine design for hepatitis C virus with meta-server and multivalent scaffolding. Sci Rep 5:12501. https://doi.org/10.1038/srep12501.
45. Sandomenico A, Leonardi A, Berisio R, Sanguigno L, Foca G, Foca A, Ruggiero A, Doti N, Muscariello L, Barone D, Farina C, Owsianka A, Vitagliano L, Patel AH, Ruvo M. 2016. Generation and characterization of monoclonal antibodies against a cyclic variant of hepatitis C virus E2 epitope 412-422. J Virol 90:3745–3759. https://doi.org/10.1128/JVI.02397-15.
46. Vietheer PT, Boo I, Gu J, McCaffrey K, Edwards S, Owczarek C, Hardy MP, Fabri L, Center RJ, Poumbourios P, Drummer HE. 2017. The core domain of hepatitis C virus glycoprotein E2 generates potent cross-neutralizing antibodies in guinea pigs. Hepatology 65:1117–1131. https://doi.org/10.1002/hep.28989.
47. Zhao L, Seth A, Wibowo N, Zhao CX, Mitter N, Yu C, Middelberg AP. 2014. Nanoparticle vaccines. Vaccine 32:327–337. https://doi.org/10.1016/j.vaccine.2013.11.069.
48. Walker LM, Burton DR. 2010. Rational antibody-based HIV-1 vaccine design: current approaches and future directions. Curr Opin Immunol 22:358–366. https://doi.org/10.1016/j.coi.2010.02.012.
49. Urbanowicz RA, McClure CP, Brown RJ, Tsoleridis T, Persson MA, Krey T, Irving WL, Ball JK, Tarr AW. 2016. A diverse panel of hepatitis C virus glycoproteins for use in vaccine research reveals extremes of monoclo-

nal antibody neutralization resistance. J Virol 90:3288–3301. https://doi.org/10.1128/JVI.02700-15.
50. El-Diwany R, Cohen VJ, Mankowski MC, Wasilewski LN, Brady JK, Snider AE, Osburn WO, Murrell B, Ray SC, Bailey JR. 2017. Extra-epitopic hepatitis C virus polymorphisms confer resistance to broadly neutralizing antibodies by modulating binding to scavenger receptor B1. PLoS Pathog 13:e1006235. https://doi.org/10.1371/journal.ppat.1006235.
51. Babcock GJ, Iyer S, Smith HL, Wang Y, Rowley K, Ambrosino DM, Zamore PD, Pierce BG, Molrine DC, Weng Z. 2014. High-throughput sequencing analysis of post-liver transplantation HCV E2 glycoprotein evolution in the presence and absence of neutralizing monoclonal antibody. PLoS One 9:e100325. https://doi.org/10.1371/journal.pone.0100325.
52. Collaborative Computational Project Number 4. 1994. The CCP4 suite: programs for protein crystallography. Acta Crystallogr D Biol Crystallogr 50:760–763. https://doi.org/10.1107/S0907444994003112.
53. Adams PD, Afonine PV, Bunkoczi G, Chen VB, Echols N, Headd JJ, Hung LW, Jain S, Kapral GJ, Grosse Kunstleve RW, McCoy AJ, Moriarty NW, Oeffner RD, Read RJ, Richardson DC, Richardson JS, Terwilliger TC, Zwart PH. 2011. The Phenix software for automated determination of macromolecular structures. Methods 55:94–106. https://doi.org/10.1016/j.ymeth.2011.07.005.
54. McCoy AJ, Grosse-Kunstleve RW, Adams PD, Winn MD, Storoni LC, Read RJ. 2007. Phaser crystallographic software. J Appl Crystallogr 40:658–674. https://doi.org/10.1107/S0021889807021206.
55. Emsley P, Cowtan K. 2004. Coot: model-building tools for molecular graphics. Acta Crystallogr D Biol Crystallogr 60:2126–2132. https://doi.org/10.1107/S0907444904019158.
56. Kleiger G, Saha A, Lewis S, Kuhlman B, Deshaies RJ. 2009. Rapid E2-E3 assembly and disassembly enable processive ubiquitylation of cullin-RING ubiquitin ligase substrates. Cell 139:957–968. https://doi.org/10.1016/j.cell.2009.10.030.